Articles

Highly Efficient Fluorene- and Benzothiadiazole-Based Conjugated Copolymers for Polymer Light-Emitting Diodes

Petra Herguth, Xuezhong Jiang, Michelle S. Liu, and Alex K.-Y. Jen*

Department of Materials Science and Engineering, Roberts Hall, Box 352120, University of Washington, Seattle, Washington 98195-2120

Received March 18, 2002; Revised Manuscript Received May 31, 2002

ABSTRACT: A series of highly efficient conjugated polymers have been synthesized for application in polymer light-emitting diodes (PLEDs). These polymers were based on the copolymerization between 9,9-dihexylfluorene and benzothiadiazole (BT). In several cases, a third comonomer was added to adjust the charge injecting and transporting properties of the polymers. All of these copolymers exhibited strong green emission at around 540 nm which can be attributed to either the charge transfer between an electron-rich segment and an electron-deficient BT-containing segment of the polymers or the Förster energy transfer between different polymer chains. These copolymers also exhibited very high photoluminescence quantum efficiencies up to 55%. A double-layer device using one of the copolymers as the emissive layer exhibited a low turn-on voltage (3.4 V), a very high external quantum efficiency (6.0%), and a high brightness of 59 400 cd/cm^2.

Introduction

Recently, fluorene-based π-conjugated polymers have emerged as a very promising candidate for polymer light-emitting diodes (PLEDs)[1] due to their combined desirable properties, such as high fluorescence quantum yield, and good film-forming and hole-transporting properties. Color tuning in these polymers can be achieved by incorporating an electron-deficient monomer, benzothiadiazole (BT), into the polymer backbone.[2−4] By incorporating BT into the fluorene polymer, the resulting copolymers possessed high electron affinity and preferential electron-transporting properties compared to those of the homopolymer, poly(9,9-dioctylfluorene) (PFO).[5] From the result of time-of-flight measurements, it showed that a fluorene-BT (1:1) copolymer, poly(9,9-dioctylfluorene-*co*-benzothiadiazole) (PBT), exhibited a strong and dispersive electron transport with the mobility of the fastest negative carriers on the order of 10^{-3} cm^2/(V s) at an applied field of 0.5 MV/cm.[5] This is almost in the same range as the highest hole mobility reported in PFO. Although PBT possesses very good electron mobility, it is a very poor hole transporter. Hole transport in PBT is highly dispersive with the carriers heavily trapped close to the surface at which they are photogenerated. To maximize the efficiency of a PLED, the ideal polymer should transport both holes and electrons equally well. However, it is a very challenging task to develop new conjugated polymers that possess both desired charge-transporting ability and still maintain the same emission energy of the fabricated devices. One possible way to circumvent this problem is to incorporate a third comonomer into the polymer backbone to provide an affective mechanism for fine-tuning the charge-transporting properties of the polymers. To facilitate the rational design of these copolymers, it is desirable to understand the role of the comonomers in affecting the polymer properties. In this paper, we report the systematic study of a series of copolymers derived from the copolymerization among 9,9-dihexylfluorene, BT, and a third electron-rich comonomer. The third electron-rich comonomer was added to adjust the charge-injecting and -transporting properties of these polymers while maintain the desirable emission colors. The electron-donating strength of the third comonomer increases in the following trend: 2,5-dimethylbenzene < dioctyloxybenzene < terthiophene. The copolymers studied in this work include poly(9,9-dihexyl-fluorene-*co*-benzothiadiazole) (9:1) PF9B, poly(9,9-dihexyl-fluorene-*co*-benzothiadiazole-*co*-(2,5-dimethyl)phenylene) (18:1:1) PF9BM, poly(9,9-dihexyl-fluorene-*co*-benzothiadiazole-*co*-(2,5-dioctyloxy)phenylene) (18:1:1) PF9BO, poly(9,9-dihexyl-fluorene-*co*-benzothiadiazole-*co*-(3-isopentyl)-2,2′:5,2-*ter*thiophene) (18:1:1) PF9BTT, and poly(9,9-dihexyl-fluorene-*co*-benzothiadiazole-*co*-(2,5-dioctyloxy)phenylene) (6:1:1) PF2BO. The electrical and spectroscopic properties of these polymers were systematically investigated. In addition, a series of double-layer PLED devices were also fabricated to study the electroluminescent (EL) properties of these polymers.

Experimental Section

Synthesis. Solvents purchased from Fisher Scientific were used as received unless stated otherwise. Toluene and tetrahydrofuran (THF) were dried over sodium and distilled. *N*,*N*-Dimethylformamide (DMF) was dried over calcium sulfate and distilled. Chemicals obtained from Aldrich or Acros were used as received.

* To whom correspondence should be addressed. E-mail: ajen@u.washington.edu.

10.1021/ma020405z CCC: $22.00
Published on Web 07/11/2002

(9,9-Dihexyl-9*H*-2,7-fluorene-diyl)bis-1,3,2-dioxoborolane was prepared following the procedures reported in the literature starting with 9*H*-fluorene.[3,6] The boronic ester was purified by recrystallization using hexane as solvent and dried under vacuum. The overall yield of the white solid was 45% (starting from 9*H*-fluorene); mp 120−122 °C. ^{1}H NMR (300 MHz, $CDCl_3$) δ (ppm): 0.75 (t, 6H, J = 7.0 Hz), 0.98−1.1 (m, 16H), 1.98 (dt, 4H, J = 4.2 Hz), 4.40 (s, 8H), 7.77 (m, 6H). ^{13}C NMR (300 MHz, ^{1}H-decoupled, $CDCl_3$) δ (ppm): 14.21, 22.72, 23.90, 29.84, 31.68, 40.50, 55.20, 66.15, 119.80, 126.63, 129.24, 133.81, 144.15, 150.67.

4,7-Dibromo-(2,1,3)-benzothiadiazole was made according to a procedure reported in the literature[7] starting with 1,2-phenylenediamine. The crude product was further purified by recrystallization in hexane. The overall yield was 61%; mp 181−183 °C (lit.[7] 184−185 °C). ^{1}H NMR (300 MHz, $CDCl_3$) δ (ppm): 7.71 (s, 2H). ^{13}C NMR (300 MHz, ^{1}H-decoupled, $CDCl_3$) δ (ppm): 114.12, 132.53, 153.16.

2,5-Di(octyloxy)benzene. Hydroquinone (10.0 g, 0.09 mol) was refluxed with octyl bromide (34.2 mL, 0.20 mol) and potassium carbonate (41.0 g, 0.27 mol) in acetone (250 mL, distilled over calcium sulfate) for 2 days. The solution was cooled to room temperature, and acetone was then evaporated under vacuum. The residue was redissolved into methylene chloride and water. The organic layer was separated, and the aqueous layer was extracted with methylene chloride. The organic layers were combined, washed with water, and dried over sodium sulfate, and the solvent was evaporated. The crude product was purified via flash column chromatography (silica gel) using hexane/methylene chloride (1:1) as eluent to afford a white solid in 67% yield; mp 56−57 °C (lit.[8] 56 °C). ^{1}H NMR (300 MHz, $CDCl_3$) δ (ppm): 0.85 (t, 6H, J = 3.6 Hz), 1.22−1.33 (m, 16H), 1.37−1.43 (m, 4H), 1.73 (dt, 4H, J = 9.0 Hz, 3.9 Hz), 3.87 (t, 4H, J = 3.9 Hz), 6.79 (s, 4H) (lit.[9]). ^{13}C NMR (300 MHz, ^{1}H-decoupled, $CDCl_3$) δ (ppm): 14.41, 22.98, 26.42, 29.61, 29.75, 32.18, 68.87, 115.63, 153.54.

1,4-Dibromo-2,5-di(octyloxy)benzene. 2,5-Di(octyloxy)-benzene (5.0 g, 0.015 mol) was dissolved in methylene chloride (50 mL), and bromine (1.7 mL, 0.033 mol) was added dropwise at room temperature. The solution was stirred in the dark at room temperature overnight. The excess bromine was quenched with a 10 wt % solution of KOH in water (50 mL). The basic layer was separated and extracted with additional methylene chloride. The organic layers were combined, washed until neutral, and then dried over sodium sulfate. The organic solvent was evaporated, and the crude product was purified via flash column chromatography (silica gel) using hexane/methylene chloride (1:1) as eluent to afford a white solid in 82% yield; mp 62−63 °C (lit.[10] 61−62 °C). ^{1}H NMR (300 MHz, $CDCl_3$) δ (ppm): 0.87 (t, 6H, J = 3.5 Hz), 1.26−1.35 (m, 16H), 1.45 (dt, 4H, J = 9.1 Hz, 4.2 Hz), 1.79 (dt, 4H, J = 9.0 Hz, 4.0 Hz), 3.92 (t, 4H, J = 3.9 Hz), 7.06 (s, 2H). ^{13}C NMR (300 MHz, ^{1}H-decoupled, $CDCl_3$) δ (ppm): 14.28, 22.86, 26.13, 29.32, 29.41, 29.45, 32.00, 70.45, 111.30, 118.59, 150.26.

3-(3′-Methylbutyl)thiophene was synthesized according to a modified literature procedure.[11] 3-Bromothiophene (14.20 mL, 0.15 mol) was added dropwise to a suspension of iodine-etched magnesium turnings (5.34 g, 0.22 mol) in diethyl ether (50 mL) at room temperature. The mixture was heated to reflux for 2.5 h. The Grignard solution was cooled to RT and then added dropwise to a solution containing 1-bromo-4-methylbutane (24 mL, 0.2 mol, distilled at 1 Pa before use) and Ni(dppp)Cl_2 (0.14 g, 0.26 mmol) in 50 mL of diethyl ether. The resulting mixture was refluxed overnight, cooled to RT, and then hydrolyzed with 1 M HCl (40 mL). The acidic layer was extracted twice with diethyl ether. All organic layers were combined, washed with water until neutral, and then dried over sodium sulfate. The solvent was removed under vacuum, and the crude residue was purified via a silica gel flash column using hexanes as the eluent to yield 15.0 g of 3-(3′-methylbutyl)thiophene (65% yield). ^{1}H NMR (300 MHz, $CDCl_3$) δ (ppm): 0.92 (d, 6H, J = 6.9 Hz), 1.50−1.57 (m, 3H), 2.63 (t, 2H, J = 7.8 Hz), 6.91 (dd, 1H, J = 2.8 Hz, 1 Hz), 6.93 (dd, 1H, J = 4.8 Hz, 0.9 Hz), 7.22 (dd, 1H, J = 4.8 Hz, 3 Hz).

2,5-Dibromo-3-(3′-methylbutyl)thiophene. The synthesis was adopted from Bäuerle et al.[12] 3-(3′-Methylbutyl)-thiophene dissolved in DMF (15 mL) was added dropwise to a solution of NBS (14.24 g, 0.08 mol) in DMF (50 mL). The solution was stirred in the dark for 3 h and then poured onto ice. The aqueous phase was extracted twice with methylene chloride. All organic layers were combined, washed with water, and dried over sodium sulfate. The organic solvent was removed under vacuum. The crude product was purified by silica gel flash column chromatography using hexane as the eluent to yield 10.2 g of dibromide in 82% yield. ^{1}H NMR (300 MHz, $CDCl_3$) δ (ppm): 0.92 (d, 6H, J = 6.9 Hz), 1.37−1.57 (m, 3H), 2.50 (t, 2H, J = 7.8 Hz), 6.76 (s, 1H).

3′-(3‴-Methylbutyl)-2,2′:5′,2″-terthiophene. The procedure used by Bäuerle et al.[12] was slightly modified for the coupling reaction. 2-Bromothiophene (9.90 mL, 0.10 mol) was added dropwise to a suspension of iodine-etched magnesium turnings (2.48 g, 0.10 mol) in diethyl ether (100 mL) at room temperature. The mixture was refluxed for 2 h. The Grignard solution was cooled to RT and then added dropwise to a solution containing 2,5-dibromo-3-(3′-methylbutyl)thiophene (12.82 g, 0.04 mol) and Ni(dppp)Cl_2 (0.14 g, 0.26 mmol) in 50 mL of diethyl ether. The solution was refluxed for 20 h, then cooled to RT, and then hydrolyzed with 1 M HCl (40 mL). The acidic layer was extracted twice with diethyl ether. All organic layers were combined, washed with water until neutral, and then dried over sodium sulfate. The solvent was removed under vacuum to yield 9.58 g of a viscous liquid (75%). ^{1}H NMR (300 MHz, $CDCl_3$) δ (ppm): 0.71 (d, 6H, J = 6.9 Hz), 1.27−1.46 (m, 3H), 2.50 (t, 2H, J = 8.1 Hz), 7.24 (dd, 1H, J = 3.6 Hz, 5.4 Hz), 7.29 (dd, 1H, J = 3.6 Hz, 5.1 Hz), 7.36 (dd, 1H, J = 1.6 Hz, 3.7 Hz), 7.38 (d, 1H, J = 1.2 Hz, 3.6 Hz), 7.43 (dd, 1H, J = 1.0 Hz, 5.2 Hz), 7.48 (s, 1H), 7.53 (dd, 1H, J = 1.0 Hz, 5.2 Hz). ^{13}C NMR (300 MHz, ^{1}H-decoupled, $CDCl_3$) δ (ppm): 22.65, 27.42, 28.23, 39.74, 123.61, 124.29, 125.31, 125.80, 126.49, 126.54, 127.47, 127.89, 129.56, 135.24, 135.97, 137.28, 140.33. MS (FAB) m/z 318.02 (calcd m/z 318.06).

5,2″-Dibromo-3′-(3‴-methylbutyl-2,2′:5′,2″-terthiophene. 3′-(3‴-Methylbutyl)-2,2′:5′,2″-terthiophene (3.19 g, 0.01 mol) dissolved in DMF (10 mL) was added dropwise to a solution of NBS (3.56 g, 0.02 mol) in DMF (50 mL). The solution was stirred in the dark for 3 h and then poured onto ice. The aqueous phase was extracted twice with methylene chloride. All organic layers were combined, washed with water, and dried over sodium sulfate. The organic solvent was removed under vacuum. The crude product was purified by a silica gel flash column with hexane as eluent to yield 3.11 g of a yellow solid; yield 65%, mp 57−58 °C. ^{1}H NMR (300 MHz, $CDCl_3$), δ (ppm): 0.93 (d, 6H, J = 6.9 Hz), 1.46−1.67 (m, 3H), 2.66 (t, 2H, J = 7.8 Hz), 8.84 (d, 1H, J = 3.6 Hz), 6.86 (d, 1H, J = 3.6 Hz), 6.90 (s, 1H), 6.94 (d, 1H, J = 3.6 Hz), 7.00 (d, 1H, J = 3.6 Hz). ^{13}C NMR (300 MHz, ^{1}H-decoupled, $CDCl_3$) δ (ppm): 22.68, 27.43, 28.26, 39.77, 111.29, 112.23, 123.89, 126.22, 126.66, 126.69, 129.05, 130.40, 130.83, 134.73, 137.29, 138.61, 141.03. MS (FAB) m/z 475.8 (calcd m/z 475.88). Anal. Calcd for $C_{17}H_{16}Br_2S_3$: C, 42.87; H, 3.39. Found: C, 42.69; H, 3.51.

Polymerization. The polymerization method was adopted from the literature.[4,6,13] The dibromoaryl and the diboronylaryl compounds were coupled via a palladium-catalyzed Suzuki-coupling reaction. Polymers were sequentially end-capped with bromobenzene and phenylboronic acid after 2 days of polymerization. The composition ratios of the polymers cited are monomer ratios used during the polymerization process. Purification was performed by repetitive fractional precipitation using THF and methanol in various ratios. The resulting polymers were air-dried overnight, followed by drying under vacuum for 8 h. The polymers were soluble in common organic solvents, such as THF, chloroform, and toluene. The number-average molecular weight of the polymers ranged from 40 to 300 kDa with a polydispersity between 1.4 and 2.0 (see Table 2).

Characterization. ^{1}H NMR and ^{13}C NMR spectra were recorded on a Bruker AF300 spectrometer in deuterated chloroform at room temperature. Melting points were deter-

Table 1. Physical Properties of the Copolymers

polymer	M_n [kDa] (M_w/M_n)	T_g [°C]	$\lambda_{max,UV}$[a] [nm]	$\lambda_{max,PL}$[a,b] [nm]	$\lambda_{max,EL}$[a] [nm]	HOMO/LUMO[c] [eV]	η_{PL}[b,d] (%)
PF9B	87.9 (1.7)	115	377 (438)	542 (561)	538, 557	−5.68/−3.67	46
PF9BO	41.7 (1.5)	115	378 (436)	540 (557)	534 (558)	−5.71/−3.16	48
PF9BTT	45.3 (1.4)	115	378 (436)	562 (540)	535 (560)	−5.63/−3.48	23
PF9BM	60.9 (1.5)	115	377 (436)	540 (561)	538 (560)	−5.69/−3.17	44
PF2BO	300.0 (2.0)	80	377 (442)	548 (560)	533	−5.66/−3.51	55

[a] Data in the parentheses are the wavelength of shoulders. [b] All polymers were excited at 378 nm. [c] HOMO/LUMO values as determined by the onset of CV measurements.[21] [d] PL quantum efficiencies in the solid state.

Table 2. Performances of Double-Layer LED Devices (ITO/HTL/Polymer/Ca/Ag)

polymer	HTL[a]	d[b] (nm)	V_{on}[c] (V)	η_{max}[d] (%)	PE_{max}[e] (cd/A)	B_{max}[f] (cd/m^2)	$V_{B_{max}}$[g] (V)	$CD_{B_{max}}$[h] (A/cm^2)
PF9B	PEDOT	70	3.4	0.90	2.65	23 800	12.6	1.62
	BTPD	70	3.6	3.7	10.9	22 800	13.8	1.57
PF9BO	PEDOT	70	3.4	0.69	2.35	8 590	14.2	1.62
	BTPD	50	3.4	2.0	5.65	9 750	13.2	1.62
PF9BTT	PEDOT	90	3.0	0.39	1.16	7 120	9.6	1.62
	BTPD	65	3.6	1.3	3.75	12 600	14.6	1.62
PF9BM	PEDOT	70	4.0	0.94	2.96	19 300	16.6	1.43
	BTPD	65	4.0	2.3	6.52	12 600	14.8	1.62
PF2BO	PEDOT	85	3.2	1.5	4.66	21 000	12.8	0.70
	BTPD	65	3.4	6.0	18.5	59 400	15.2	1.62

[a] Hole-transporting layer (BTPD = BTPD-PFCB). [b] Thickness of the emitting layer. [c] Turn-on voltage (defined as the voltage required to give a luminance of 1 cd/m^2). [d] Maximum external quantum efficiency. [e] Maximum photometric power efficiency. [f] Maximum brightness. [g] Operating voltage at the maximum brightness. [h] Current density at maximum brightness (1.62 A/cm^2 was set as the maximum current density allowed in the instrument).

mined on a electrothermal melting point apparatus. FAB-MS spectra were recorded with nitrobenzoic acid as matrix. The molecular weight of the polymers was determined by gel permeation chromatography (Waters, Styragel HR 4E) with THF (HPLC grade, Fisher Scientific) as eluent (flow rate 0.5 mL/min) and polystyrenes as external standards. Cyclic voltametric data were measured on a BAS CV-50W voltametric analyzer using tetrabutylammonium perchlorate (0.1 M) in acetonitrile (electrochemical grade, Fisher Scientific) as electrolyte and indium tin oxide (ITO) and Ag/Ag^+ as the working and reference electrode, respectively. Data were recorded from polymer films spin-cast onto ITO substrates at a scan rate of 100 mV/s with ferrocene as the external standard. The glass-transition temperature (T_g) was taken from differencial scanning calorimetry graphs recorded on a Shimatzu DSC-60 under nitrogen with a scan rate of 10 °C/min. UV−vis absorption spectra were measured using a Perkin-Elmer Lambda 9 UV/vis/NIR spectrophotometer. Photoluminescence (PL) data were recorded with an Oriel InstaSpec IV charge coupled device (CCD). PL efficiencies of polymer films on quartz substrates were measured using the CCD camera in combination with a Newport integrating sphere,[14] with monochromated light from a Hg lamp as the excitation source. Films used for the PL efficiency measurement were drop-coated from toluene solution onto quartz substrate (1−5 wt %).

Light-Emitting Device Fabrication and Testing. The light-emitting devices were prepared on commercial ITO-coated glass substrates (Colorado Concept Coating), which had been ultrasonicated sequentially in a detergent solution, deionized water, methanol, 2-propanol and acetone, and treated with O_2 plasma for 10 min before use. Either PEDOT (polyethylene dioxythiophene: polystyrene sulfonate, purchased from Bayer Corp.) or an in-situ polymerized polymer, bis(tetraphenyldiamino)biphenyl−perfluorocyclobutane (BTPD-PFCB),[15,16] was used as the hole-transporting layer. The PEDOT layer was spin-coated at a spin rate of 4000 rpm from an aqueous solution (1.3 wt %) onto the pretreated ITO substrates and cured at 160 °C for 10 min under nitrogen. The hole-transporting layer of BTPD-PFCB was generated by spin-coating its monomer solution (1 wt % in 1,2-dichloroethane) at 2000 rpm and followed by curing at 225 °C for 45−60 min.[15,16] The emissive layer was then spin-coated on top of the hole-transporting layer from a toluene solution of the copolymers (1 wt %) with a spin rate of 1400 rpm. The thickness of the organic layer was measured on a Sloan Dektak 3030 surface profiler. The thickness of the HTL was ∼35−40 nm, and the thickness of the copolymer layer was ∼65−90 nm (Table 2). Then a 30 nm thick of the Ca cathode was deposited in a vacuum evaporator inside an argon atmosphere drybox, at a pressure of $\sim 1 \times 10^{-6}$ torr. An additional layer of Ag (120 nm) to be used as a protecting layer was then evaporated on top of the Ca layer under the same condition as Ca. The device testing was carried out in air at room temperature. The current−voltage characteristics of the devices were measured on a Hewlett-Packard 4155B semiconductor parameter analyzer. EL emission power was measured using a Newport 2835-C multifunction optical meter in combination with a calibrated photodiode. Photometric data were calculated using the emission power and EL spectra of the devices, assuming the Lambertian distribution of the EL emission.[17]

Results and Discussion

The physical properties of the copolymers are summarized in Table 1. The number-average molecular weight of the copolymers range from 40 000 to 300 000 as determined by gel permeation chromatography and the T_g from 80 to 115 °C. The increasing content of the dialkoxyphenylene groups in PF2BO decreases the T_g of this polymer due to its long alkyl chains that plasticize the polymer.

Spectroscopic Properties. The absorption and luminescence maxima of the copolymers are very similar (Figure 2). All polymers exhibited an absorption λ_{max} at 378 nm and a luminescence maximum at 540 nm with a vibronic peak at 560 nm. In the cases of PF9B, PF9BO, PF9BTT, and PF9BM, the absorption at 378 nm can be attributed to the polyfluorene part of the polymer. In fact, it was previously demonstrated that the effective conjugation length of a ∼6−8 unit fluorene oligomer will account for an absorption wavelength around this region (376−380 nm).[18] This suggests that BT and the third comonomers are randomly distributed among the fluorene blocks with more than six fluorene units in between. In the case of PF2BO, it seems that the polyfluorene−octyloxyphenylene part is the main contributing unit in the polymer that is responsible for the absorption. From the literature, a poly(fluorene−octyloxyphenylene) alternating copolymer was reported previously to have an absorption λ_{max} at 380 nm.[19]

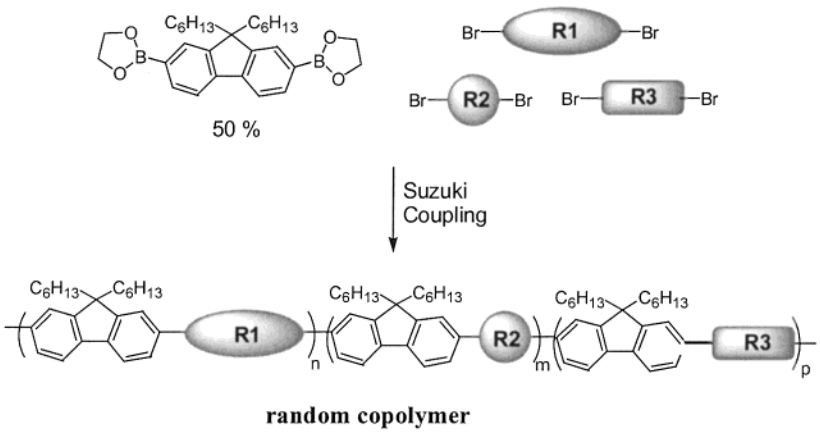

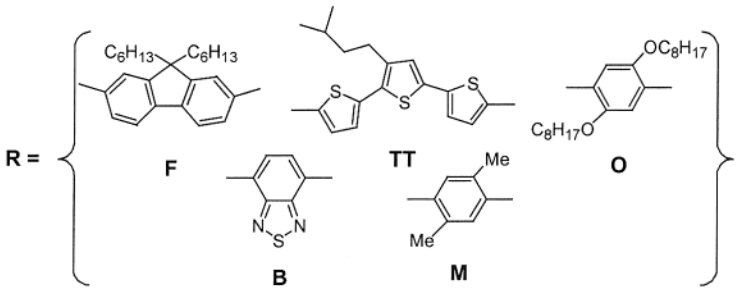

Polymer	R1	R2	R3	Total % of fluorene (**F**)
PF9B	**F** - n = 40	**B** - m = 10	---	90 %
PF9BO	**F** - n = 40	**B** - m = 5	**O** - p = 5	90 %
PF9BTT	**F** - n = 40	**B** - m = 5	**TT** - p = 5	90 %
PF9BM	**F** - n = 40	**B** - m = 5	**M** - p = 5	90 %
PF2BO	**F** - n = 25	**B** - m = 12.5	**O** - p = 12.5	75 %

Figure 1. Synthesis and composition of polymers.

When a BT unit was incorporated into the polymer backbone at a concentration even as low as 10% in the case of PF9B, a red-shifted luminescence peak was observed when compared with polyfluorene.[20] The energy calculated from the PL was close to that observed for the alternating poly(fluorene benzothiadiazole) copolymer PBT.[20] This indicated that the electron-deficient BT unit tends to dominate the luminescence properties through the charge-transfer effect between an electron-rich segment and an electron-deficient BT-containing segment of the polymers or through the Förster energy transfer between different polymer chains by functioning as an acceptor. By copolymerizing fluorene with BT and a third comonomer, such as 2,5-dimethylbenzene (PF9BM), 2,5-dioctyloxybenzene (PF9BO), or 3′-(3‴-methylbutyl)-2,2′:5′,2″-terthiophene (PF9BTT), the polymer properties can be further fine-tuned. In these cases, the BT and the fluorene content were kept constant; only the third component was varied. All the resulting copolymers also exhibited similar absorption and emission properties (Figure 2). Excitation of these polymers at either their absorption peak (λ_{exc} = 377 nm) or at their shoulder (436 nm) resulted in a strong emission at 542 nm with a broad shoulder at 560 nm. From the large Stokes shift observed when the polymers were excited at 377 nm, strong evidence was presented for efficient energy transfer from the higher energy oligofluorenes part to a lower energy BT-containing site of the polymers. For PF9BTT, the first vibronic peak at 560 nm became the main peak, which might be due to the higher thiophene content of the copolymer. None of the polymers emitted light in the blue range, where polyfluorene was expected to have its emission maximum (around 425 and 445 nm).[20] Thus, the emission properties of these polymers seem to be dominated by charge transfer or energy transfer to the BT-containing sites of the copolymer. Even a relatively small BT content (5%) in polymers such as PF9BO, PF9BTT or PF9BM shifted the PL peak completely to a longer wavelength than the homopolymer (Figure 2). This suggested that the BT-containing sites of the polymer possess the lowest energy level. On the other hand, it seems that the third comonomer in these copolymers does not have any influence on the emission wavelength of the polymer.

The absorption properties of PF2BO and PF9BO are quite similar. They both have an absorption λ_{max} at 377 nm, but PF2BO has a more prominent shoulder at 442 nm (Figure 2). The increase in intensity of the shoulder can be attributed to the increase in BT content from

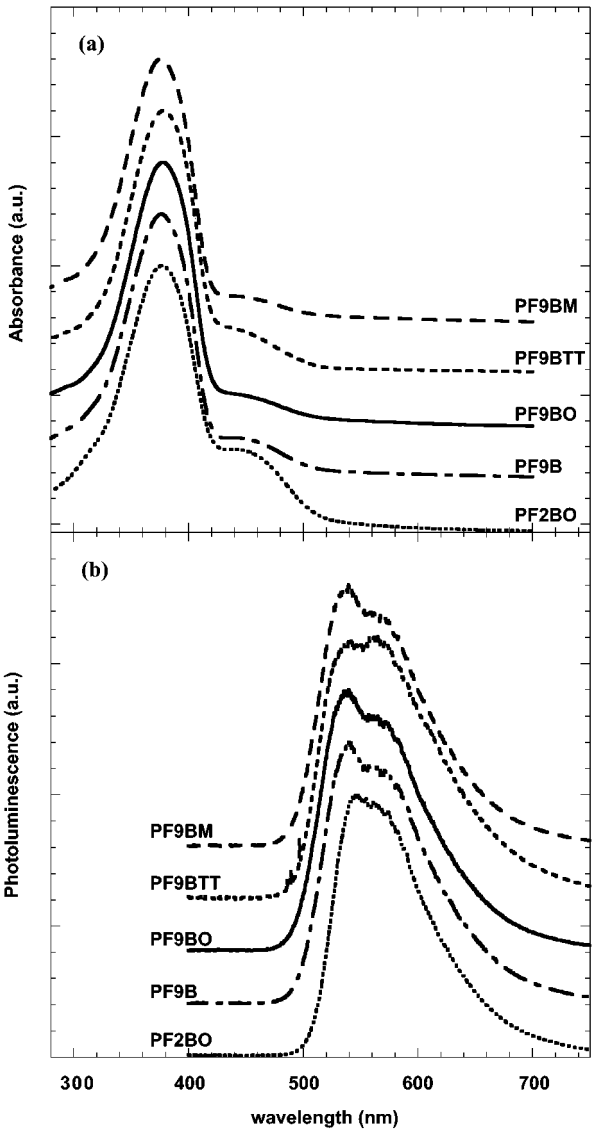

Figure 2. Absorption (a) and PL (b) spectra of PF2BO (···), PF9B (– –), PF9BO (—), PF9BTT (- - -), and PF9BM (– – –). Data were recorded from the spin-coated films on quartz substrates. Spectra are normalized to the highest data point. For the PL measurement, all polymers were excited at 378 nm.

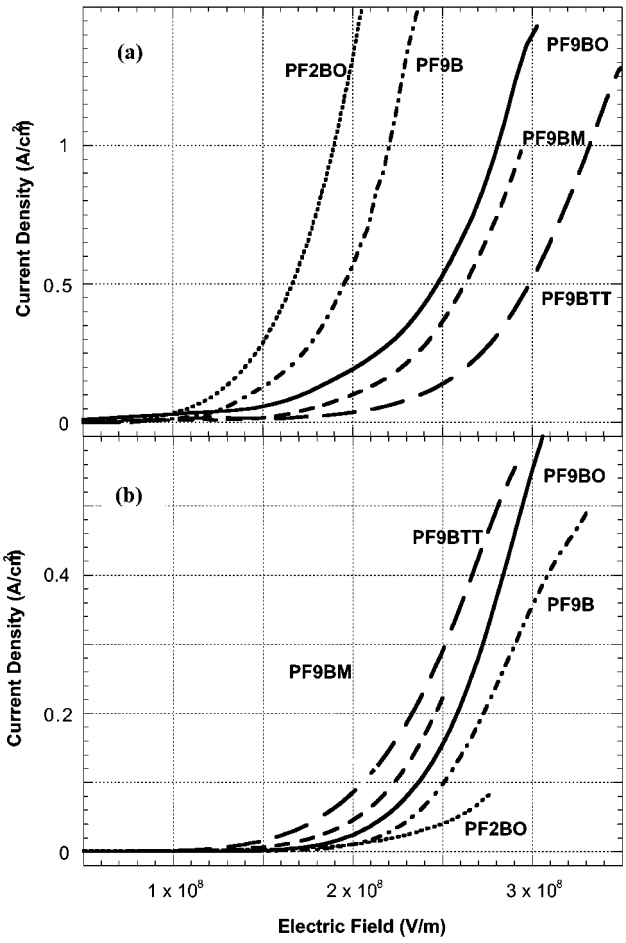

Figure 3. *I*–*V* curves for (a) electron-only (ITO/Al/polymer/Ca/Ag) and (b) hole-only (ITO/polymer/Au) devices: PF2BO (···), PF9B (– · –), PF9BO (—), PF9BTT (– – –), and PF9BM (– - –).

5% to 12.5%. The position of the main emission peak is slightly red-shifted from 540 nm in PF9BO to 548 nm in PF2BO. This may be due to an intramolecular charge-transfer between the dialkoxyphenylene and the BT units.

The PL quantum efficiency of the copolymers is ranging from 23% for PF9BTT to 55% for PF2BO (Table 1). With the exception of PF9BTT, the PL efficiency of the polymers is quite similar (44–55%). Thus, the incorporation of a third comonomer into the polymer backbone also only had a slight effect on the PL quantum efficiency of the copolymers except in the case of PF9BTT, whose third comonomer contained a ter-thiophene ring. The heavy atom effect from the sulfur on the thiophene ring may increase the intersystem crossing of singlet to triplet which results in the loss of PL efficiency.

Charge Transport Properties. Although the emission color of the copolymers were not influenced by either BT concentration or the content of the third comonomer, it did alter the energy levels of the copolymers, as can be seen from the redox potentials obtained by cyclic voltammetry (Table 1). In most of the cases, the LUMO levels are affected by the presence of the third comonomer. In addition to the modification of the LUMO energy level, the charge mobility of the copolymers was also dependent on the third comonomer that was used. Figure 3 showed the *I*–*V* curves of the copolymers. Among the three copolymers of PF9BO, PF9BTT, and PF9BM, PF9BTT possessed the highest hole conductivity as it was shown from the tests of the hole-only devices. However, it also possessed the lowest electron conductivity. This is due to that the ter-thiophene unit with its electron-rich five-membered ring tends to facilitate hole transport but inhibits electron transport (Figure 3).

When the charge-transporting properties of PF2BO and PF9BO were compared, these two polymers possessed comparable hole conductivity, but PF2BO with a higher BT content showed a much higher electron conductivity. The higher electron conductivity in PF2BO may contribute significantly to the improved LED device performance since a more balanced charge transport can be achieved in devices fabricated with this polymer.

Electroluminescent Properties. The EL performance of the copolymers was examined using a double-layer device configuration of ITO/HTL/polymer/Ca, where HTL was either PEDOT or the in-situ polymerized BTPD-PFCB. The performance of the devices was summarized in Table 2. When compared with the PL

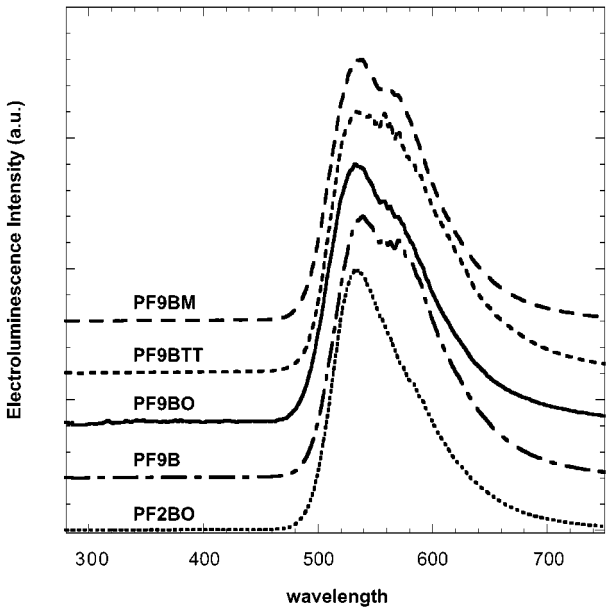

Figure 4. EL spectra of PF2BO (···), PF9B (– –), PF9BO (—), PF9BTT (- - -), and PF9BM (– – –) from ITO/BTPD-PFCB/polymer/Ca/Ag devices run at 7−8 V.

maximum of the polymers in Table 1, the EL maximum of the resulting devices is slightly blue-shifted, but their vibronic fine structures were conserved except in the case of PF2BO (Figure 4). The morphology of the PF2BO device might be different due to higher molecular weight of the polymer, thus depressing the 0−1 vibronic transition. The PL and EL quantum efficiencies of the copolymers followed a similar trend with PF9BTT possessing not only the lowest efficiency in both PL and EL with 23% and 3.1%, respectively, but also showed the lowest brightness in the trisegment copolymer category. The oligomeric thiophene may contribute significantly to the deactivation pathways of quenching luminescence in the device.

Among all the devices tested, the best device was the one made with the configuration of ITO/BTPD-PFCB/PF2BO/Ca/Ag. It exhibited a very large external quantum efficiency (6.0%) and photometric power efficiency (28.6 cd/A) at an operating voltage of 3.6 V (Table 2). The device also possessed the highest brightness (59 400 cd/m^2) among all devices tested. Figure 5 showed the *I*−*V*−*L* curves of the two devices fabricated with PF2BO as the emissive layer. However, when PEDOT was used as the HTL, the devices exhibited both lower brightness and stability compared to the devices made with BTPD-PFCB as the HTL. The external quantum efficiency of the devices using BTPD-PFCB as the hole-transporting layer is also 3−10 times higher than that of the devices using PEDOT as the hole-transporting layer. This could be due to two reasons: (1) a better planarized interface between ITO and the emissive polymer and (2) a balanced charge injection and transport achieved by using the BTPD-PFCB as the HTL.

Conclusion

We have synthesized a series of fluorene-based polymers with various ratios of electron-rich and electron-deficient moieties as comonomers to improve their charge injecting and transporting properties. High PL quantum efficiencies of up to 55% were observed for these materials. LEDs made of these polymers exhibited high external quantum efficiencies (0.69−6.0%) and

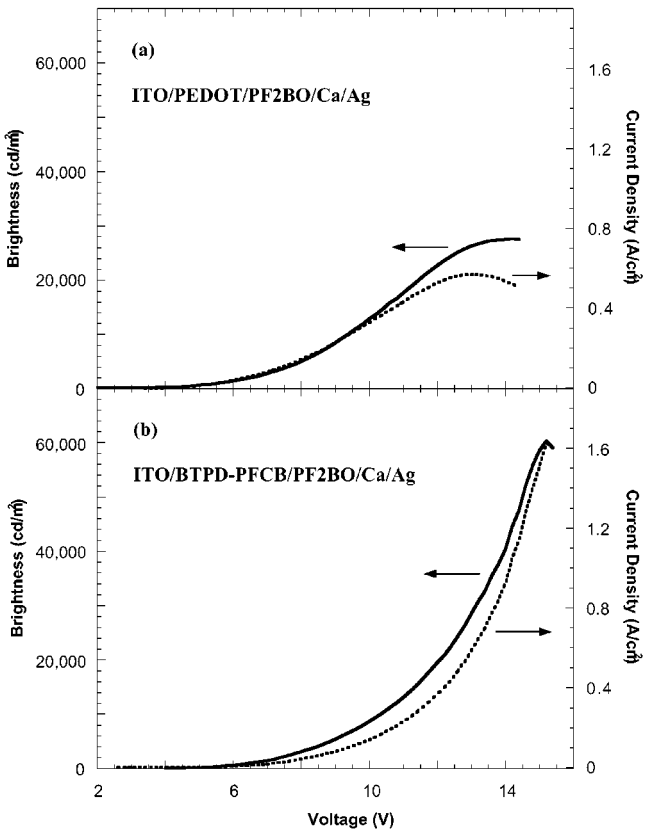

Figure 5. *I*−*V*−*L* curves {(—) brigthness; (···) current density} for devices with the configuration (a) ITO/BTPD-PFCB/PF2BO/Ca/Ag and (b) ITO/PEDOT/PF2BO/Ca/Ag.

high photometric power efficiency (as high as 28.6 cd/A). A maximum brightness of 59 400 cd/cm^2 was observed for the device fabricated with PF2BO as the emissive layer. The results from PL, EL, and conduction measurements showed that the optical and electrical properties of the copolymers could be fine-tuned by adjusting the copolymerization ratio and electron-rich or -deficient nature of the comonomers.

Acknowledgment. The authors thank the Air Force Office of Scientific Research (AFOSR) for their support through the MURI Center (Polymeric Smart Skins) and the DURIP Program. A.J. thanks the Boeing-Johnson Foundation for financial support. M. Liu thanks the Nanotechnology Center at the University of Washington for the Nanotechnology Fellowship.

References and Notes

(1) Bernius, M. T.; Inbasekaran, M.; O'Brien, J.; Wu, P. *Adv. Mater.* **2000**, *12*, 1737.
(2) Donat-Bouillud, A.; Blondin, P.; Ranger, M.; Bouchard, J.; Leclerc, M. *Chem. Mater.* **2000**, *12*, 1931.
(3) Inbasekaran, M.; Woo, E. P.; Wu, W.; Bernius, M. T. WO00/46321, 2000.
(4) Inbasekaran, M.; Woo, E. P.; Wu, W. WO99/20675, 1999.
(5) Campbell, A. J.; Bradley, D. D. C.; Antoniadis, H. *Appl. Phys. Lett.* **2001**, *79*, 2133.
(6) Inbasekaran, M.; Wu, W.; Woo; E. P. US 5,777,070, 1998.
(7) Pilgram, K.; Zupan, M.; Skiles, R. *J. Heterocycl. Chem.* **1970**, *7*, 629.
(8) Hartley, G. S. *J. Chem Soc.* **1939**, 1828.
(9) Loupy, A.; Sansoulet, J.; Diez-Barra, E.; Carrillo, J. R. *Synth. Commun.* **1991**, *21*, 1465.
(10) Vahlenkamp, T.; Wegner, G. *Macromol. Chem. Phys.* **1994**, *195*, 1933.
(11) Lemaire, M.; Garreau, R.; Garnier, F.; Roncali, J. *New J. Chem.* **1987**, *11*, 703.

(12) Bäuerle, P.; Pfau, F.; Schlupp, H.; Würthner, F.; Gaudl, K.; Caro, M.; Fischer, P. *J. Chem. Soc., Perkin Trans. 2* **1993**, 489.
(13) Towns, C. R. WO00/53656, 2000.
(14) Mello, J. C.; Wittmann, H. F.; Friend, R. H. *Adv. Mater.* **1997**, *9*, 230.
(15) Jiang, X.; Liu, S.; Liu, M. S.; Ma, H.; Jen, A. K.-Y. *Appl. Phys. Lett.* **2000**, *76*, 2985.
(16) Liu, S.; Jiang, X.; Ma, H.; Liu, M.; Jen, A. K.-Y. *Macromolecules* **2000**, *33*, 3514.
(17) Greenham, N. C.; Friend, R. H.; Bradley, D. D. C. *Adv. Mater.* **1994**, *6*, 491.
(18) Klaerner, G.; Miller, R. D. *Macromolecules* **1998**, *31*, 2007.
(19) Yu, W.-L.; Pei, J.; Cao, Y.; Huang, W.; Heeger, A. J. *Chem. Commun.* **1999**, 1837.
(20) Buckley, A. R.; Rahn, M. D.; Hill, J.; Cabanillas-Gonzales, J.; Fox, A. M.; Bradley, D. D. C. *Chem. Phys. Lett.* **2001**, *339*, 331.
(21) According to the redox onset potentials of the CV measurements, the HOMO/LUMO energy levels of the polymers were estimated on the basis of the reference energy level of ferrocene (4.8 eV below the vacuum level): LUMO/HOMO = $-(E_{onset} - 0.12\ eV) - 4.8\ eV$, where the value 0.12 eV is for ferrocene vs Ag/Ag^{+}.

MA020405Z